

Recent advances in flexible fiber-shaped metal-air batteries

Lei Ye, Yang Hong, Meng Liao, Bingjie Wang^{**}, Dacheng Wei, Huisheng Peng^{*}, L. Ye, Y. Hong, M. Liao, B. Wang, D. Wei, H. Peng

Laboratory of Advanced Materials, State Key Laboratory of Molecular Engineering of Polymers, and Department of Macromolecular Science, Fudan University, Shanghai, 200438, China

ARTICLE INFO

Keywords:

Fiber-shaped battery
Metal-air battery
Flexible metal anode
Flexible cathode
Gel electrolyte

ABSTRACT

Metal-air batteries in fiber shape, which are theoretically endowed with high energy densities, have emerged as a versatile platform for the advance of next-generation flexible electronics. The past decade has witnessed the booming development of fiber-shaped metal-air batteries including flexible lithium-air (oxygen) batteries, zinc-air batteries, aluminum-air batteries and lithium-CO₂ batteries. Here the recent advances of fiber-shaped metal-air batteries are briefly summarized, with particular emphasis on the fabrication of flexible electrodes, the electrolyte exploitation and encapsulating material optimization. The remaining challenges and promising directions are highlighted to provide clues for the practical implementation of fiber-shaped metal-air batteries.

1. Introduction

Flexible energy storage devices have been widely explored to satisfy the next-generation electronic devices that are thin, lightweight, flexible and even stretchable [1–4]. Some prototypes of advanced electronics in need of flexible energy storage devices, such as Huawei Mate X flexible smartphone, Samsung Youm flexible display and wearable Apple Watch, also recently appear [5–8]. They are expected to not only shape the future consumer electronic products but also open up new areas including wearable electronics, biomedical devices, and artificial intelligence in the near future [9–12]. The main attentions are previously paid to making the energy-storage devices as thin as possible to achieve the desiring flexibility [13–15]. As a result, they may easily break during fabrication and use. In addition, although they can be bended, it is challenging for them to bear twisting and other more complex deformations in three dimensions. Furthermore, they are not breathable and comfortable particularly for some boosting fields like wearable electronics [16–18].

A new family of 1D fiber-shaped energy storage devices thus attracts increasing interests in the past decade [19–21]. They can be woven into energy storage textiles that are thin, lightweight, highly flexible and even stretchable to bear severe and complex deformations. The resulting energy storage textiles are breathable and comfortable [22]. It is also effective for them to be integrated into emerging smart systems that need

to be miniaturized on the basis of well-developed weaving method [23–26]. Lithium ion batteries were first made into a fiber shape due to the ease in fabrication [25]. However, the low energy densities have largely limited their real applications despite of a lot of efforts that are made to enhance them.

The other types of batteries have been thus extensively studied in just a few years. Among them, metal-air batteries are mostly investigated for much higher energy densities than lithium-ion batteries [27–32]. For instance, theoretical energy density of Li–O₂ batteries reaches 3600 Wh·kg⁻¹ [33–37] in comparison to 460 Wh·kg⁻¹ [38] for Li-ion batteries. Moreover, considering the characteristic half-open system that contains air (mainly referring to O₂) as cathode material from the environment, we may find some interesting and promising advantages in them. For instance, a 360° solid-liquid-air interface in the fiber-shaped metal-air battery promotes ion transfer with O₂ in air as the reactant, and it is particularly useful for the resulting energy storage textiles [20]. The recent development in fiber-shaped metal-air batteries is summarized with a brief chronology in evolution (Fig. 1). The main advances are made from three key parts of flexible electrodes, electrolytes and sealing materials. Therefore, here we carefully review this field by summarizing the synthesis, structure and property of the above three types of materials. The remaining challenges and possible directions in fiber-shaped metal-air batteries are highlighted to provide useful insights for the future development.

* Corresponding author.

** Corresponding author.

E-mail addresses: wangbingjie@fudan.edu.cn (B. Wang), penghs@fudan.edu.cn (H. Peng).

<https://doi.org/10.1016/j.ensm.2020.03.015>

Received 14 January 2020; Received in revised form 6 March 2020; Accepted 13 March 2020

Available online 21 March 2020

2405-8297/© 2020 Elsevier B.V. All rights reserved.

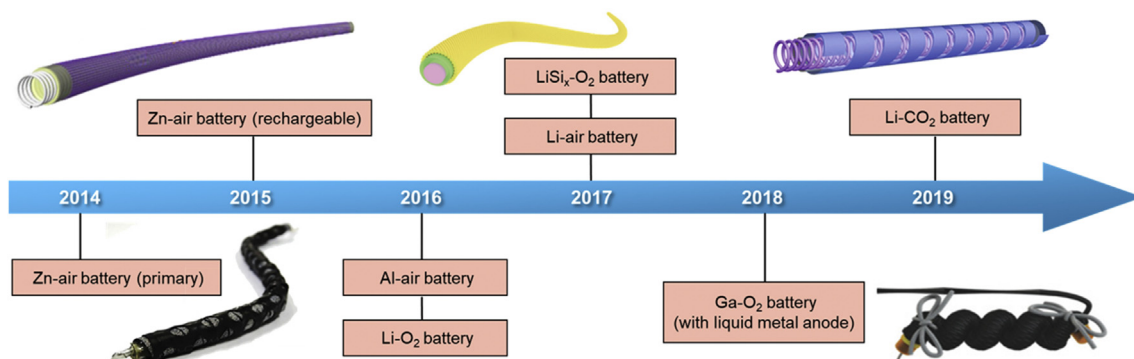


Fig. 1. A brief chronology of the development of fiber-shaped metal-air batteries [45,72,91,112,115]. Reproduced with permission [45,72,91,112,115]. Copyright 2015, 2017, 2018, Wiley-VCH.

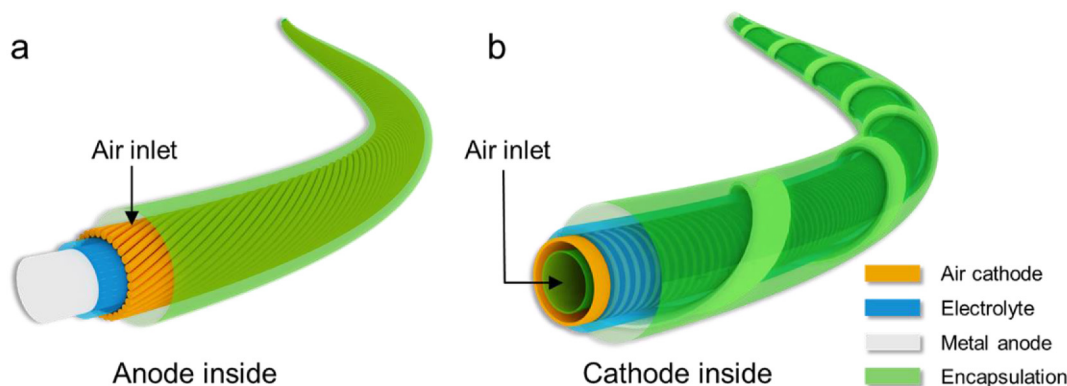
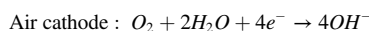


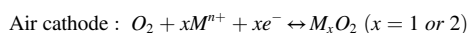
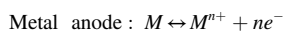
Fig. 2. Schematic presentation for two types of fiber-shaped metal-air battery configurations, i.e., anode inside a) and cathode inside b).

2. Device configurations

The development of fiber-shaped metal-air batteries is always premised on the advance of flexible electrodes. Different from fiber-shaped lithium ion batteries and supercapacitors with diverse configurations such as twisting and parallel structures [39–44], flexible electrodes for fiber-shaped metal-air batteries, namely, air cathodes and metal anodes, are preferred to be constructed in a coaxial configuration [21]. This is determined by the varying reaction mechanisms of metal-air batteries. For metal-air batteries with aqueous electrolytes, the discharge processes are as follows ($M = \text{Zn}/\text{Al}/\text{Mg}/\text{Fe}$):



The metal ions released from metal anode react with OH^- in aqueous electrolyte to form $M(\text{OH})_n$ and meanwhile the oxygen from environment is reduced to OH^- at the catalyst layer in cathode [29]. For metal-air batteries with aprotic electrolytes, the reaction processes could be concluded as below ($M = \text{Li}/\text{Na}/\text{K}$):



The discharge/charge reactions rely on the reversible stripping/plating process in metallic anodes. And in air cathodes, the ORR/OER is the reversible formation and decomposition of superoxide or peroxide, depending on the battery type [33]. As for the newly conceptual Li-CO₂ batteries, the anode reaction is the same as Li-O₂ battery while CO₂ is employed instead of O₂ as the cathode reactant and the discharge product

is Li₂CO₃ and C [45]. In general, both flexible air cathode and metal anode depend on reaction mechanisms involving the ambient air/O₂ as indispensable reactant and thus the coaxial structure can afford maximized area for gas adsorption compared with other types of assembly configurations (e.g., twisted or parallel structures) for fiber-shaped batteries [20,46].

To date, the coaxial architectures for 1D metal-air batteries can be divided into two categories according to the assembly scheme: anode-inside and cathode-inside batteries as depicted in Fig. 2. In anode-inside metal-air batteries (Fig. 2a), the 1D metal anode is first constructed, and then wrapped by an air cathode layer separated with gel electrolyte between them [47]. This structure shares several benefits: (i) the inner metal anode is covered in a multi-layer manner, thus effectively preventing its corrosion by ambient moisture or gas; (ii) the outer air cathode layer with relatively larger diameter can be fully exposed to surrounding air for improved reaction current density. As for cathode-inside metal-air batteries (Fig. 2b), air cathodes are often constructed in a central ventilation structure to allow air inlet, and the flexible metal wire/strips coated with electrolyte are then wrapped around as the anode outside [45]. This prototype is promising for metal-air batteries that require pure oxygen as the source, which can be directly pumped from the gas container into tubular air cathodes.

3. Air cathodes

In metal-air batteries, the oxygen reduction reaction (ORR) and oxygen evolution reaction (OER) primarily take place in the air cathode, which is composed of electrochemical active materials and porous current collectors [48–50]. Generally, a suitable air cathode utilized for 1D metal-air batteries should simultaneously possess high catalytic activity, flexibility, and mechanical properties to achieve high specific energy

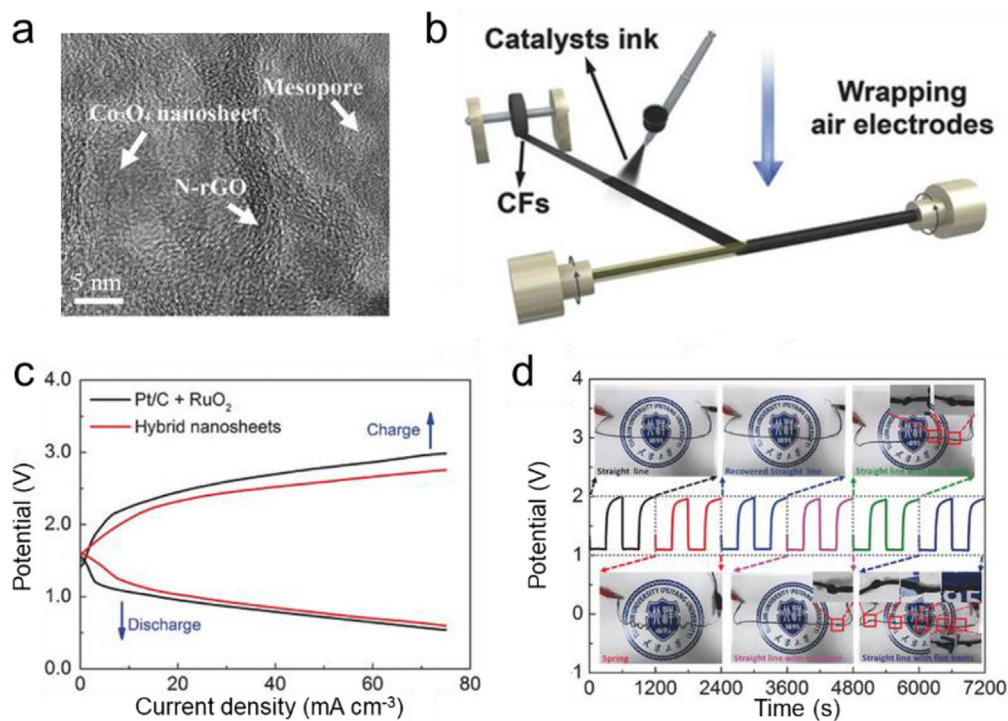


Fig. 3. a) HRTEM image of atomically thin mesoporous Co₃O₄/N-rGO hybrid nanosheet catalyst. b) Spray-coating process for preparing the air cathode of fiber-shaped Zn-air battery. c) Discharge and charge polarization curves of fiber-shaped Zn-air batteries with Co₃O₄/N-rGO hybrid nanosheet and commercial Pt/C + RuO₂ cathodes. d) Galvanostatic discharge and charge curves of fiber-shaped Zn-air battery under various shapes [55]. Reproduced with permission [55]. Copyright 2018, Wiley-VCH.

density with high structural stability [51,52]. There exist some nice review articles on squeezing the capacity of oxygen redox catalysts, so we here focus on the fabrication strategies (i.e., spray/cast-coating and *in-situ* synthetic methods) of air cathodes designed for 1D flexible metal-air batteries.

3.1. Spray/cast-coating methods

The spray/cast-coating method is a popular strategy to obtain flexible

air cathodes, which also proves effective for a wide range of 1D metal-air batteries. In a representative work, a mixture slurry of 90 wt% SP and 10 wt% PVDF was brushed onto flexible carbon textile current collectors to fabricate flexible air cathode, which was then wrapped around a Li rod separated with gel electrolyte to avoid the short circuit [53]. As a result, the cable-type Li–O₂ battery could stably work under various bending and twisting deformations, demonstrating both high flexibility and mechanical stability. Sharing the similar fabrication process, the sulfur-doped CaMnO₃ nanotubes treated by calcination and sulfurization

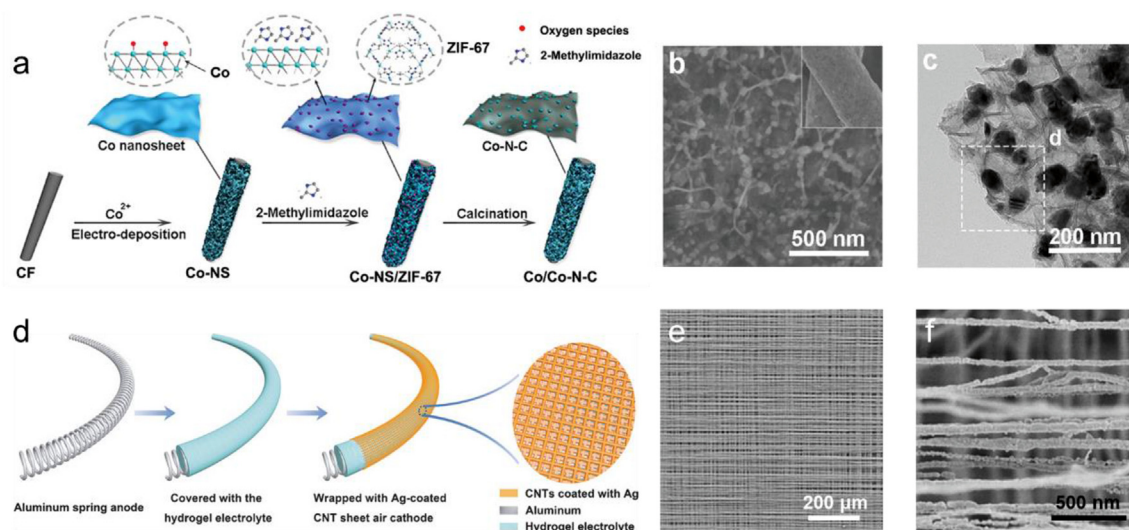


Fig. 4. a) Schematic of the fabrication for free-standing Co/Co-N-C air cathode. b, c) SEM and TEM images of the Co/Co-N-C air cathode [63]. Reproduced with permission [63]. Copyright 2019, Wiley-VCH. d) Schematic of the fabrication process for fiber-shaped Al-air battery containing Ag-coated CNT sheets air cathode. e, f) Corresponding SEM images of the Ag-coated CNT sheets air cathode at low and high magnification, respectively [71]. Reproduced with permission [71]. Copyright 2016, Wiley-VCH.

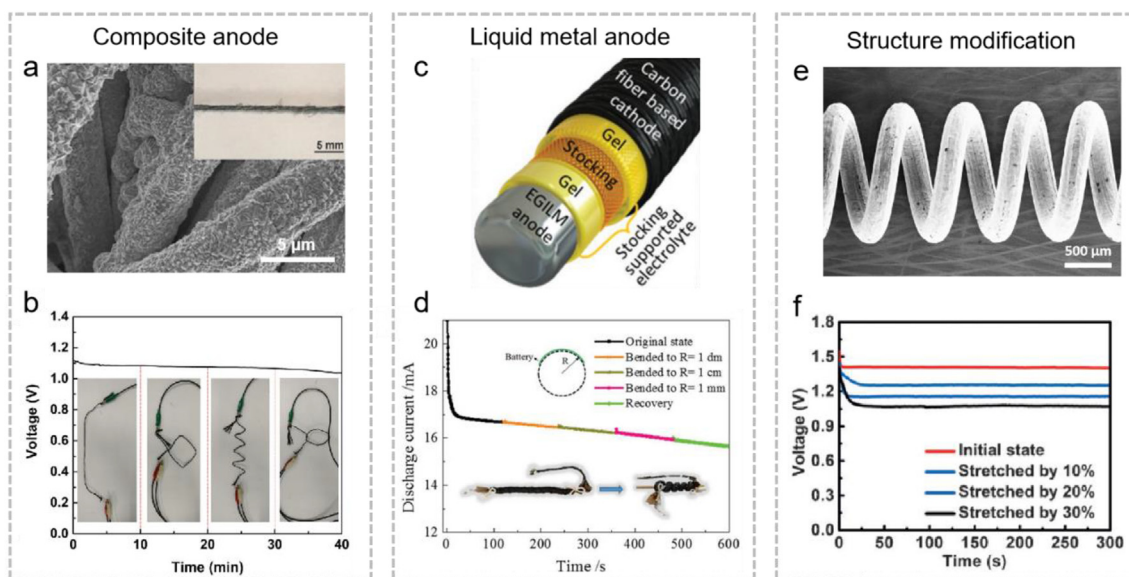


Fig. 5. a) SEM and photograph of a Zn-plated yarn fiber. b) Discharge curve of fiber-shaped Zn-air battery at a current density of $1.6 \text{ mA}\cdot\text{cm}^{-3}$ under varying deformations [89]. Reproduced with permission [89]. Copyright 2018, Wiley-VCH. c) Schematic illustration of fiber-shaped Ga/In- O_2 battery. d) Discharge curve of fiber-shaped Ga/In- O_2 battery with various curvature radiuses [91]. Reproduced with permission [91]. Copyright 2018, Wiley-VCH. e) SEM image of a spring-like metal wire [72]. f) Discharge curves of the fiber-shaped Al-air battery under different stretching states at a discharge current of 1 mA [71]. Reproduced with permission [71]. Copyright 2016, Wiley-VCH.

were mixed with carbon black and Nafion solution to form a uniform slurry, followed by a casting procedure onto carbon cloth to construct flexible air cathode for Zn-air batteries [54].

The merits from the simple procedure of spraying/casting method become more apparent when we consider the continuous fabrication of flexible air cathodes. A prototype for scalable production of flexible air cathode was demonstrated by continuously spray-coating the catalyst ink onto Toray carbon fibers (Fig. 3a and b) [55]. To obtain the catalyst ink, a bifunctional catalyst composed of the atomically thin mesoporous 2D $\text{Co}_3\text{O}_4/\text{N-rGO}$ hybrid nanosheets was synthesized and then uniformly dispersed into solution. The state-of-art fabrication method realized fiber-shaped Zn-air batteries with high volumetric energy density of $36.1 \text{ mWh}\cdot\text{cm}^{-3}$, which could be knitted into normal textiles for power supply (Fig. 3c and d). Despite of the above advances, the spray coating method inevitably requires extra additives, including binders and conductive agents, to prepare the slurry/ink for the spray coating procedure. However, some of the involved additives like PVDF and PTFE prove unstable in the oxygen-rich environment [56–58], thus deteriorating the electrochemical performances of fiber-shaped metal-air batteries. Besides, due to the multi-component feature in the prepared slurry, the indirect contact between the active material and current collector is undesirable for the ORR/OER kinetics and the mechanical integrity against deformations [59,60].

3.2. In-situ fabrication methods

The free-standing cathodes obtained by *in-situ* synthesis of active materials on flexible substrates are considered more suitable with following advantages. First, 1D flexible metal-air batteries are ideally constructed in compact structures with high aspect ratio and high radius of curvature, which magnify the difficulty in forming a homogeneous active material layer by spray/cast coating methods [61]. In this aspect, direct growth of active materials ensures a much more uniform layer for ORR/OER reactions. Second, due to the strong combination between *in-situ* synthesized active material and current collectors, improved structural stability and mass transfer are available [62]. As an intriguing attempt, by means of synthesizing Co nano-islands rooted on the Co nanosheets through *in-situ* synthesis, hybrid air cathodes with sufficient

active sites and effective electron/ionic transport for catalytic reactions were accomplished (Fig. 4a) [63]. The *in-situ* formed, conductive network bridging high OER performance catalyst and flexible carbon felt substrate (Fig. 4b and c) endowed the obtained fiber-shaped Zn-air battery with stable discharge/charge voltage profiles upon bending deformations and small discharge-charge polarization gap (0.82 V at $10 \text{ mA}\cdot\text{cm}^{-2}$), revealing the promoted electron/mass transport. One further step, utilizing the electrospinning technique to prepare self-standing air cathodes by *in-situ* synthesizing N-doped carbon flake arrays on the carbon nanofibers, the researchers observed increased cycling stability of 90 cycles at $1.25 \text{ mA}\cdot\text{cm}^{-2}$ [64]. Based on the controllable chemical composition, air permeability and scalable potential of electrospinning nanofibers [65–67], it is envisioned that this technology could implement more designed flexible electrodes and deserves more efforts for 1D batteries.

Aligned carbon nanotube (CNT) sheets, benefited from their high flexibility, light weight ($\sim 1.41 \mu\text{g}\cdot\text{cm}^{-2}$), good conductivity ($10^4\text{--}10^5 \text{ S}\cdot\text{cm}^{-1}$) and high specific surface area ($\sim 424.4 \text{ m}^2\cdot\text{g}^{-1}$) [68–70], could afford facilitated gas diffusion channels and abundant reaction sites for electrochemical reactions, and thus have greatly contributed to the exploitability of *in-situ* synthesized flexible air cathode in 1D metal-air batteries. In the first place, the aligned CNT with ORR/OER activities was directly used as air cathode for Li- O_2 batteries [47]. Attempts have been made to wrap aligned CNT sheets as air cathode around a Li wire anode coated with gel electrolyte, achieving a fiber-shaped Li- O_2 battery with high specific capacity of $12,470 \text{ mAh}\cdot\text{g}^{-1}$ based on the cathode mass. The porous structure and good mechanical properties of aligned CNTs provided large space to accommodate insoluble discharge product (Li_2O_2) during discharge process and thus yielded a highly durable 1D battery structure against over 100 bending cycles. Distinct from its effective utilization in Li- O_2 batteries with organic electrolyte, the pristine CNT shows poor ORR activity in aqueous solution [71]. In pursuit of enhanced catalytic capability of the air cathode in aqueous electrolytes and expanded applications toward more battery chemistries (e.g., Al-air batteries), Ag nanoparticles were uniformly deposited on the cross-stacked CNT bundles by thermal evaporation deposition (Fig. 4d–f) [71]. The Ag/CNT composite exerted a positive influence on catalytic activities of the fiber-shaped Al-air battery, making much lower

polarization and improved capacity over $1000 \text{ mAh}\cdot\text{g}^{-1}$ at $0.5 \text{ mA}\cdot\text{cm}^{-2}$. Along with the innovations of CNT-based 1D Al-air batteries, the RuO_2 -incorporated aligned CNT was also developed to fabricate high-performance air cathode for fiber-shaped Zn-air batteries [72].

The chemical stability of substrates or current collectors in air cathodes is crucial to the performance of batteries. Despite of the above advantages of carbon substrates, in some cases that require high charge overpotentials (e.g., Li-air batteries), the irreversible side reactions rising from the instabilities of carbon in the presence of highly oxidative product would produce insoluble side products, block the air cathode and lead to inferior electrochemical performances [60,73,74]. These problems could be effectively remitted by replacing the carbon substrate with metal-based current collector. By employing the stainless-steel mesh as substrate for *in-situ* growth of N-doped CNTs (N-CNT) [75], a Li-air battery fiber was achieved with an exceptional cycle stability of ~ 232 cycles and a good rate performance ($\sim 4000 \text{ mAh}\cdot\text{g}^{-1}$ at $2000 \text{ mA}\cdot\text{g}^{-1}$). It is noteworthy that, besides the metal substrate, N-CNTs with high graphitization degrees also contributed to high stability in oxygen-rich environment [76,77]. Similarly, direct incorporation of active materials onto metallic fiber substrates also showed enhanced stability in 1D Li-CO₂ battery, where a N-CNT network was synthesized on a flexible Ti wire as the air cathode [45,78].

4. Flexible metal anodes

At early stage, metal rods and wires have been directly used as flexible anodes for fiber-shaped metal-air batteries due to the certain deformability of metal including Li, Na, Zn and Al [79,80]. It should be pointed out that only limited flexibility can be achieved for pure metal, which is far from satisfying the demands of 1D flexible metal-air batteries. Additionally, the charge storage of anode in metal-air batteries generally relies on the reversible metal (e.g., Li, Na and Zn) stripping/plating process, which is always plagued by the corrosion and dendrite growth associated with severe safety problems [81–84]. To this end, a lot of efforts mainly focused on the synthesis of flexible composite anodes, the configuration designs and the fabrication of alloy anodes have been made to solve the above problems.

Most metals, e.g., Zn, suffer from the shape memory effect, making monolith metal wire/rods incapable of withstanding continuous bending [85–88]. Therefore, to meet the requirements of 1D metal-air batteries, the composite metal anodes in 1D format, by introducing intrinsically flexible substrates, were prepared to enhance the flexibility for frequent deformations such as bending and twisting [21,22]. As shown in Fig. 5a, a flexible and robust fiber-shaped Zn anode was prepared by uniformly coating a cotton yarn with Cu metal by electroless plating and then electrodeposition of Zn metal [89]. The flexible nature of cotton yarn, together with the strong adhesion between Cu and the coated Zn layer, enabled highly stable structure and good electrochemical performance over 75 cycles at $3 \text{ mA}\cdot\text{cm}^{-3}$ of the resulting Zn-air battery fiber in a coaxial architecture. Notably, these yarn-based battery fibers demonstrated high flexibility comparable to traditional fibers, and no significant performance decay was observed upon twisting and knotting into complex shapes (Fig. 5b).

The introduction of lightweight and flexible substrate not only enhances the flexibility but also reduces the mass of excess metal (e.g., Zn), thus contributing to a higher integral energy density. More recently, a scalable roll-electrodeposition approach was highlighted because of its realization of continuously fabricating fiber-shaped Zn anodes on the basis of aligned CNT fibers [90]. Inherited from good mechanical properties of aligned CNTs, the fiber-shaped Zn anodes could be optimized with high structural integrity and designed into double-helix structure to further improve the flexibility. Apart from incorporating metals onto flexible substrates, the use of liquid metal to construct flexible metal anode represents an interesting concept and has recently been proposed [91]. Room temperature liquid metal was injected into a flexible, cannular cavity and utilized as anode for 1D metal-air battery (Fig. 5c).

The 1D liquid metal (90 wt% of gallium and 10 wt% of indium) anode delivered high flexibility and elasticity, enabling effortless recovery from varying deformations of bending or twisting. Notably, the discharge current of the battery fiber remained nearly unchanged during the bending and recovery operations with curvature radii ranging from 10 to 1 mm (Fig. 5d).

Considering the real-world applications, high durability of 1D flexible metal-air battery against complex deformations, for example, stretching, is required. Although many metals demonstrate good ductility, the metal rod/wire/foils are not stretchable. A facile structure design method for stretchable metal anodes is to wind the metal wire in a spiral manner to form spring-like metal anode (Fig. 5e) [72]. The obtained spiral structure alleviates the local stress concentration and thus endows the metal anode enhanced stretchability upon a variety of applied stress [71,72]. The fiber-shaped Zn-air/Al-air batteries could be stretched by up to 30% on the basis of the spring-like Zn/Al metal anodes without electrochemical performance degradation (Fig. 5f). The spring-like metal anode could also afford large contact area with electrolyte for enhanced interfacial stability, which enacted as a 98% maintained open circuit voltage of the fiber-shaped Al-air battery after continuous bending for 1000 cycles. Although structure modification is effective, the enhancement of flexibility and stretchability of metal wire/rods from this method is relatively limited. And the resulting fiber-shaped metal-air batteries generally demonstrated less compact structure due to the large diameter ($>2 \text{ mm}$) of the spring-shaped anodes.

Compared with metallic Zn and Al with high stability in air, Li metal is highly reactive and flammable [92]. Besides, the use of flammable organic electrolyte in 1D flexible Li-air batteries further increases the difficulty of fabrication and operation [93]. Therefore, main efforts have been devoted to improve the stability and prevent the corrosion of reactive metallic Li anode to avoid safety risks. Noting that designing novel electrolyte and encapsulating materials are helpful for Li stabilizing, which would be detailedly discussed in following sections. In view of the fabrication of flexible Li anodes, one promising strategy to thoroughly settle the safety issues from Li/Na metals is replacing them with high capacity and non-metallic anodes, such as alloy-type compounds M_xLi ($\text{M} = \text{Si, Ge, Sn, Al, etc.}$) [30,94]. In a representative work, a lithiated silicon/CNT hybrid fiber was designed as the anode for 1D Li-air battery [46]. The Si nano-particles were first introduced into aligned CNT fibers via a co-spun method, followed by lithiation through an electrochemical alloying process. Due to the absence of excessive usage of Li metal, this hybrid fiber anode not only avoided severe safety problems and dendrite formation of Li metal, but also showed high flexibility. A high energy density of $512 \text{ Wh}\cdot\text{kg}^{-1}$ was achieved based on the total weight of two electrodes with a compact coaxial architecture and the Li-air battery fiber exhibited stable performance after 20,000 bending cycles. Sharing the similar strategy, lithiated Al-carbon and Sn-carbon anodes have also been explored to replace the pure Li metal for Li-air battery with high safety and flexibility [95,96]. More efforts should be made to expand the alloy systems and explore the relationship between structure and property in them for high performance anodes in the future.

5. Electrolytes

The electrolyte in metal-air batteries serves as a crucial medium for the transport of metal ions and oxygen during charge and discharge. Non-liquid electrolytes with free-standing features are preferred since 1D flexible metal-air batteries with liquid electrolytes are prone to leak upon repeated deformations, resulting in the failure of battery and even safety problems [97,98]. Furthermore, an eligible electrolyte system for fiber-shaped metal-air battery should satisfy several essential requirements including high ionic conductivity, high oxygen solubility and diffusibility, high electrochemical stabilities, good coordination with other components of battery and high flexibility [99,100]. With this in mind, the quasi-solid polymer-based gel electrolytes are promising for 1D

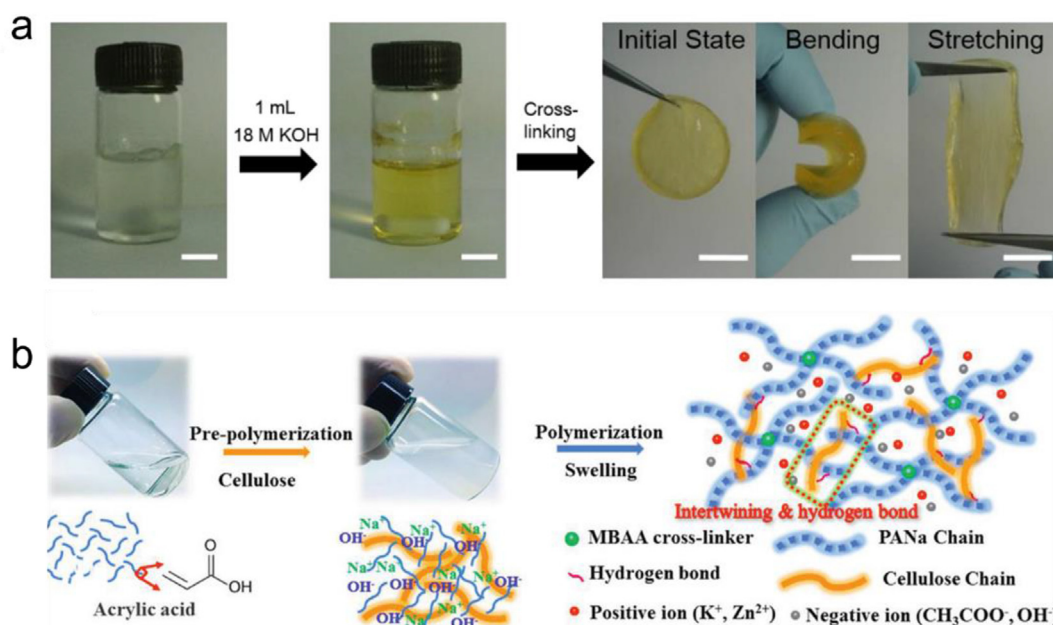


Fig. 6. a) Preparation procedures of flexible PVA-PEO-KOH gel polymer electrolyte [72]. b) Schematic of the fabrication for super-stretchable PANa-cellulose hydrogel electrolyte [110]. Reproduced with permission [110]. Copyright 2019, Wiley-VCH.

flexible metal-air batteries with promising advantages. First, the gel electrolytes relieve the problems of volatilization or leakage that occurred for liquid electrolytes, thus enabling high flexibility against various deformations. Second, their quasi-solid feature aids in the suppression of dendrite growth as well as the avoidance of internal short circuit [101]. Third, gel electrolytes with hydrophobicity can prevent the highly active metal from the corrosion of moisture or CO_2 in ambient air [53,102,103]. These merits are expected to yield high electrochemical performance and flexibility for 1D metal-air batteries with both aqueous and organic electrolyte systems.

5.1. Aqueous electrolytes

Aqueous gel polymer electrolytes (GPEs) or hydrogels containing alkaline hydroxide salts (e.g., KOH, LiOH and NaOH) and polymer frameworks were mostly utilized for 1D Zn-air and Al-air batteries [104, 105]. These hydrogels with decent kinetic, intrinsic flexibility and mechanical stability were highly compatible to the flexible 1D batteries [106,107]. Generally, aqueous GPEs are prepared by swelling the polymer hosts with suitable aqueous solutions, followed by the addition of concentrated aqueous alkaline solutions which are capable of forming stable gel with other components in the batteries. The as-prepared GPE can be directly coated onto the flexible electrodes for the construction of 1D metal-air batteries after proper evaporation process. In preparing the aqueous GPE, KOH is usually preferred compared with other alkaline salts due to its desirable ionic conductivity, relatively low viscosity, large oxygen diffusion coefficient, and good solubility of carbonate byproduct [104]. The GPE was previously prepared by dissolving PVA into the aqueous KOH solution under continuous stirring [108]. The obtained PVA-KOH- $\text{Zn}(\text{OAc})_2$ gel was then applied to the electrodes *via* brush painting for several times to fabricate the cable-like Zn-air battery, which could stably work upon varying bending angles from 0 to 90° . A modified new GPE with improved mechanical properties (could be stretched for up to 300%) and ionic conductivity ($0.3 \text{ S}\cdot\text{m}^{-1}$) was later developed by adding poly(ethylene oxide) (PEO) into KOH-PVA based GPE (Fig. 6a) [72]. Remarkably, the unchanged discharge voltage after 100 bending and stretching cycles indicated high flexibility of the 1D Zn-air battery inherited from this modified GPE. The application scope of KOH-PVA electrolyte was then expanded to 1D Al-air battery fiber by introducing

ZnO into GPEs, which effectively remitted the Al corrosion [71].

In above electrolyte systems, GPEs were generally prepared individually, and then incorporated with flexible electrodes. Considering the high viscosity of GPEs, the interfacial contacts between GPEs and electrodes are relatively poor, leading to large cell resistance and easy detachment once encountering an intensive deformation. In this regard, *on-site* formed gel electrolyte for 1D flexible metal-air batteries may enable improved interfacial contacts with both anode and cathode [109]. For instance, Liu and co-workers took advantages of the *in-situ* polymerization of polyacrylic acid (PAA) to synthesize GPE and then utilize it for a novel fiber-shaped Ga/In-air battery [91]. The liquid polymeric precursor solution was first paved onto the anode with seamless contact, followed by the polymerization at room temperature. By tuning the chain length of PAA, they had optimized the GPE for high tensile elongation up to 205.6% with a recovery rate of $>99.5\%$. Successively, a PANa-cellulose dual-network hydrogel electrolyte characterized by its super stretchability was developed recently (Fig. 6b) [110]. The abundant chemical and physical cross-linking designed in this GPE contributed to facilitated energy dissipation and highly durable structure against strain. As a result, the fiber-shaped Zn-air battery achieved an elongation up to 500% without electrochemical performance decay. This strategy had been also modified with the use of biomass materials to demonstrate a success in planar metal-air batteries [111]. Inspired by the former triumph, Park and co-workers had exploited a natural gelation as gelling agent for *in-situ* formation of the GPE, for the construction of 1D Zn-air battery [112]. Due to its high ionic conductivity ($3.1 \times 10^{-3} \text{ S}\cdot\text{cm}^{-1}$), the biomass GPE demonstrated comparable solution and charge transfer resistance with those of the liquid electrolytes, thus affording facilitated kinetics in 1D Zn-air batteries.

5.2. Organic electrolytes

Due to the combination of promising features including high solubility of oxygen and lithium salt, high ionic conductivity and especially, good stability with highly reactive Li metal, organic GPE systems are generally employed for 1D flexible Li-air batteries [99]. As discussed before, different from Zn or Al, metallic Li is flammable and prone to be corroded by moisture or CO_2 from the ambient air [113]. Thus, the key to prepare GPE for 1D flexible Li-air batteries should focus on not only

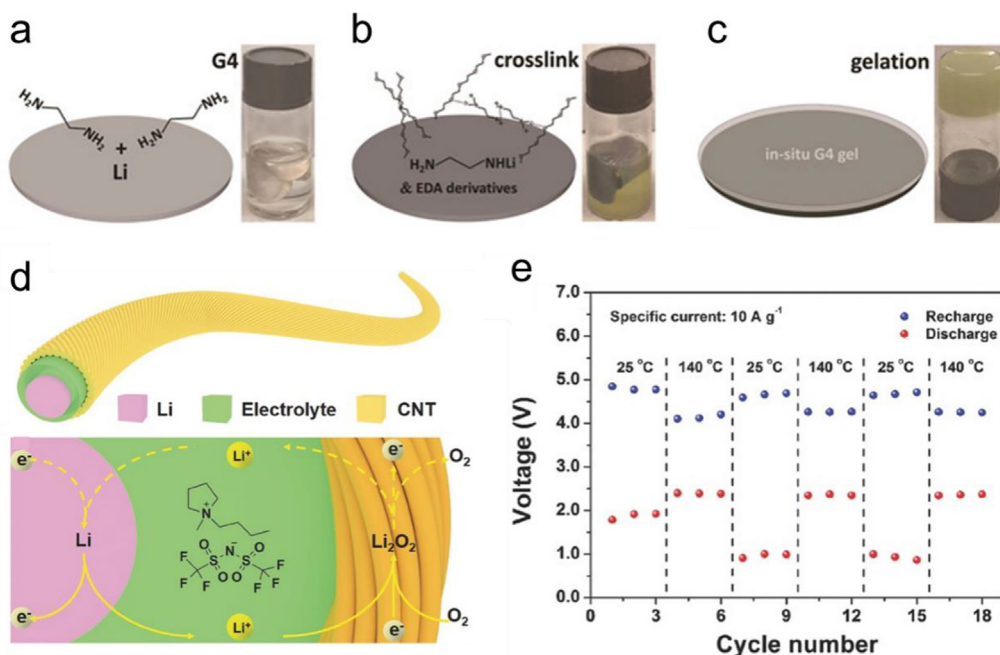


Fig. 7. a-c) Schematic and preparation procedures for self-gelling TEGDME electrolyte [114]. Reproduced with permission [114]. Copyright 2018, Wiley-VCH. d) Schematic of fiber-shaped Li-air battery with high thermal stability up to 140 °C. e) Variation of discharge and charge voltage plateaus under varying temperatures of 25 and 140 °C [115]. Reproduced with permission [115]. Copyright 2018, Wiley-VCH.

preventing electrolyte leakage and short circuit upon repeated deformation during usage, but also improving the moisture resistance and the protection of Li metal. To this end, a freestanding GPE comprising of 1 M LiTF in TEGDME and PVDF-HFP/ethoxylated trimethylolpropane-triacrylate (ETPTA)-based framework was developed for 1D Li–O₂ battery [53]. The hydrophobic GPE effectively prevented the penetration of moisture into the battery and thus protected the lithium anode from corrosion, yielding a cable-type Li–O₂ battery that could stably work after immersed in water for 5 h. An *in-situ* self-gelling GPE without additional gelling agent had been further explored in pursuit of more simplified and efficient electrolyte systems [114]. Through the gradual reaction of TEGDME with LiEDA on the Li metal surface, the liquid TEGDME electrolyte with 1% ethylenediamine (EDA) was gelatinized to form a protection layer (Fig. 7a–c). This self-gelling reaction ensured good interfacial contact with Li metal, which was favorable for the prevention from moisture and CO₂. The longevity for over 50 days of the resulting

Li-air battery fiber in ambient air with humidity of 45–65% further indicated the effective protection by the self-gelling GPE, outperforming those with liquid electrolytes.

Promising as above organic GPEs are, several improvements are still required to deal with the complex usage conditions of 1D metal-air batteries. For example, despite of its adsorption in polymer frameworks, the vaporization of organic solvents in GPEs may still occur, especially under elevated temperatures, resulting in the formation of flammable gases and unstable electrochemical performances [99]. Therefore, it is necessary to expand the operating temperature range of GPEs, particularly when we consider the open architecture of 1D metal-air batteries. In this regard, room temperature ionic liquids, with negligible vapor pressure, wide electrochemical window, low flammability and high thermal stability are preferred for the preparation of GPEs [115]. To this end, a novel GPE system employing ionic liquid that could provide effective protection for Li metal at a high temperature of 140 °C

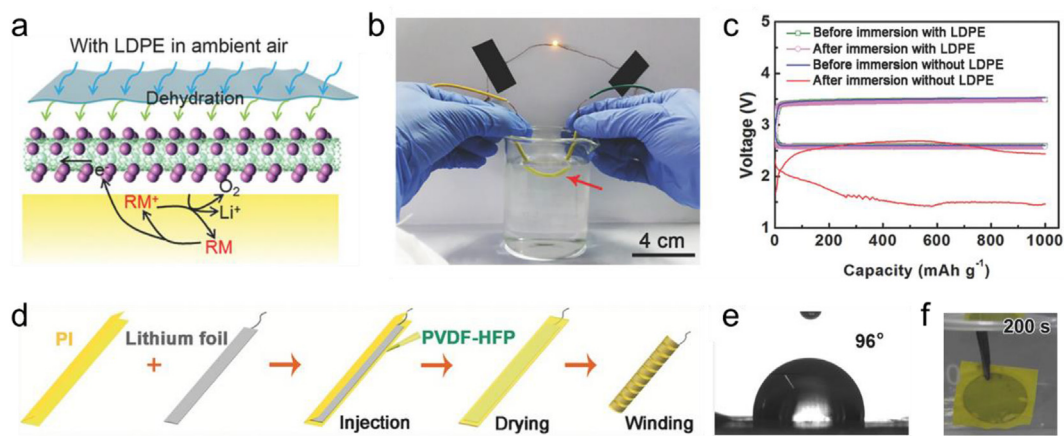


Fig. 8. a) Schematic of the working mechanism of fiber-shaped Li-air battery with LDPE encapsulation in ambient air. b) Stable operation of a fiber-shaped Li-air battery immersed in water. c) Corresponding discharge and charge voltage profiles of the batteries before and after immersion in water [121]. Reproduced with permission [121]. Copyright 2018, Wiley-VCH. d) Schematic of the fabrication for a flexible PIPV-encapsulated Li anode. e) Water contact angle of PIPV film. f) Stability of a PIPV-encapsulated Li metal immersed in water [122]. Reproduced with permission [122]. Copyright 2018, Wiley-VCH.

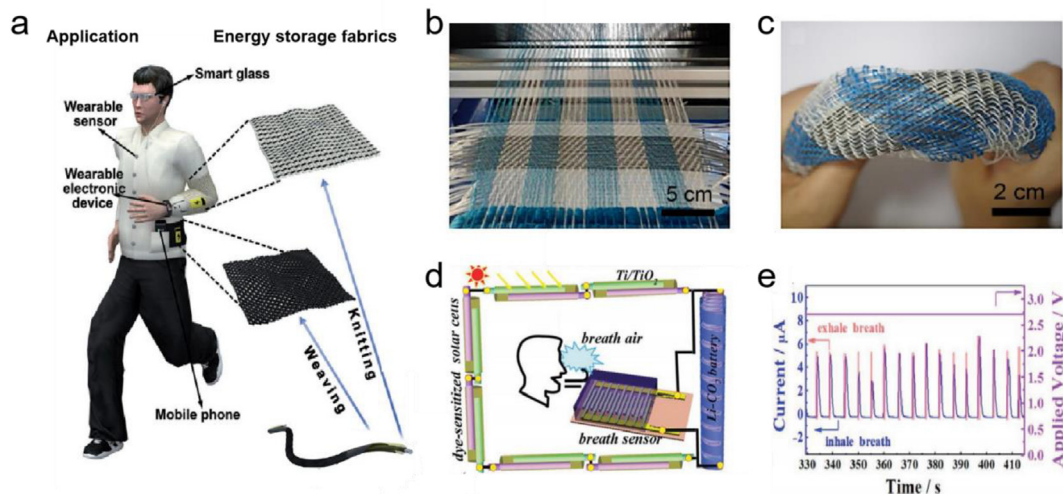


Fig. 9. a) Schematic illustration for the applications of fiber-shaped metal-air batteries [55]. Reproduced with permission [55]. Copyright 2018, Wiley-VCH. b) Photograph showing the process of fiber-shaped Li-air batteries being woven into energy fabrics. c) Photograph of the flexible energy textile under twisting [46]. Reproduced with permission [46]. Copyright 2017, Wiley-VCH. d) Schematic presentation of a self-powered breath monitor consisting of energy harvester, energy storage and response device. e) The repeated dynamic response performance of the breath monitor [45]. Reproduced with permission [45]. Copyright 2019, Wiley-VCH.

was proposed (Fig. 7d) [116]. All components in the GPE exhibited good thermal stability under high temperature, and enhanced ionic conductivities from 10^{-4} to 10^{-3} S·cm $^{-1}$ were observed under increasing temperatures from 25 to 100 °C, indicating lower inner resistance and therefore better rate performance upon elevated temperature (Fig. 7d). The obtained fiber-shaped Li-air battery, as expected, demonstrated a high cycling stability over 350 cycles and excellent rate capability durable of current density up to 10 A·g $^{-1}$ at 140 °C (Fig. 7e). Besides a lot of efforts made to design electrolytes for Li-air batteries operated at high temperatures, some attempts are also made to enhance the electrochemical performances of electrolytes at low temperatures (e.g., at -70 °C), which is critical for the practical application of 1D flexible Li-air batteries [117]. More attentions should be paid to synthesize electrolytes that may work at low temperatures or better work at a broad range from high to low temperatures.

6. Encapsulation materials

For the practical implementation of 1D flexible metal-air batteries, flexible electrodes along with GPEs should be properly encapsulated. Considering the unique features of 1D flexible metal-air batteries, we have to overcome two key challenges mainly in view of structural and functional requirements [52]. First, the selected encapsulating material should possess good flexibility, proper mechanical strength and relatively low mass density so as to maintain high structural integrity of 1D metal-air batteries durable of various deformations. Second, in regard with the battery reactions involved in the half-open architectures, the encapsulation should be highly compatible against other components and accessible of oxygen into the air cathode while preventing the undesired diffusion of moisture or CO $_2$ into the batteries. To date, aluminum-plastic films [118], thermoplastic materials [47], and poly(ethylene terephthalate) (PET) [119] have been employed as the encapsulation for 1D and other types of flexible metal-air batteries including Zn-air, Al-air and Li-air batteries.

The above-mentioned encapsulating materials have easy availability and high flexibility, but most of them could only be applied to laboratory-scale metal-air batteries, with pure dry oxygen supply. However, for the real-world applications of 1D metal-air batteries, a robust and open battery system using the surround air, is highly desirable. Wang and co-workers took a great leap forward producing a Li-air battery fiber with ultralong cycle life in ambient air by utilizing low-density polyethylene

(LDPE) as encapsulating material (Fig. 8a) [120]. The LDPE film with nonpolar structure exhibited high selectivity for nonpolar O $_2$ molecules and effective isolation against polar H $_2$ O molecules with an extremely low H $_2$ O permeability at 0.825 g·m $^{-2}$ ·d $^{-1}$. With the protection of LDPE, the as-prepared fiber-shaped Li-air battery could be operated in ambient air with relative humidity of ~50% and achieved long cycle life of over 600 cycles (Fig. 8b and c). Similarly, the silicone oil, which could function as O $_2$ -selective medium, was introduced into the hydrophobic PVDF-HFP film to encapsulate 1D Li-air battery, and an increased capacity of 640 mAh·g $^{-1}$ was successfully achieved in air [121]. To further guarantee the safe usage of Li anode, a polyimide and poly(vinylidene fluoride-co-hexafluoropropylene) composite (PIPV) film was designed (Fig. 8d and c) [122]. The wrapped flexible Li strip could be directly immersed in water, demonstrating desirable stability (Fig. 8f). Moreover, an outmost, thermotolerant heat-shrinkable tube was optimized for the encapsulation of the integral Li-air battery cable, further preventing the electrolyte from combustion even under exposure to flame.

7. Applications

For practical applications of fiber-shaped metal-air batteries, one promising direction is wearable power textiles (Fig. 9a) [55]. With flexibility, breathability and stable

electrochemical performances, they can not only serve as power supply for electronics but also provide a highly compatible platform for various techniques. Previously, fiber-shaped Al-air and Li-air batteries (lengths of centimeters) were woven into a piece of existing fabric to power electronics such as wrist bands and backpacks [47,71]. Following with that, more powerful textiles had been obtained by sewing up fiber-shaped Zn-air batteries containing the commercially available Zn wire anodes. Due to the high conductivity of Zn wire, the knittable Zn-air battery fiber with a total length of ~30 cm could maintain stable electrochemical performances. And the resulting power textiles could stably work without short circuits under external forces [55].

For the weaving or knitting fabrication of power textiles directly from fiber-shaped batteries, rigorous criteria are required for the building of fiber-shaped metal-air batteries. For instance, they should be thin enough to be qualified for the weaving/knitting techniques where the natural/synthetic yarns for cloths were generally with diameter of only 200–300 μ m. Due to their multi-layered, coaxial structures, however, metal-air battery fibers were generally thick with diameters of millimeters [22].

Table 1
Materials and properties of representative fiber-shaped metal-air batteries.

Type	Air cathode		Anode	Electrolyte	Battery performance	Flexibility evaluation	Ref
	Catalyst	Current collector					
Zn–O ₂ battery	Co ₃ O ₄ /N-rGO	Carbon fiber	Zn wire	PVA-KOH	75 cycles 0.5 mAh·cm ⁻³	Knittable	[55]
	Co ₃ O ₄	Carbon fiber yarn	Zn plated cotton yarn	PVA-KOH	24 cycles 0.27 mAh·cm ⁻³	Knittable	[89]
	PPy-GR@ZIF-8	CNT paper	Zn spring	PANa-cellulose-KOH	300 cycles 0.23 mAh·cm ⁻²	Stretching by 500%.	[110]
	RuO ₂	Aligned CNT sheet	Zn spring	PVA-PEO-KOH	30 cycles 500 mAh·g ⁻¹	Bending/stretching for 100 cycles	[72]
	Fe/N/C	Carbonized silk fibroin	Zn spring	Gelatin-KOH	Primary 1 mAh·cm ⁻²	Bendable	[112]
	Co ₄ N/Co–N–C	Carbon cloth	Zn spring	PVA-KOH	36 cycles 0.83 mAh·cm ⁻²	Bending/stretching for 2000 cycles	[62]
	Co/Co–N–C	Carbon felt	Zn wire	PVA-KOH-Zn(OAc) ₂	60 cycles 0.17 mAh·cm ⁻³	Bendable	[63]
Li–O ₂ battery	SP	Carbon textile	Li wire	PVDF-HFP/ETPTA-LiTF-TEGDME	90 cycles 500 mAh·g ⁻¹	Bendable	[53]
	Ru@CNT	Carbon textile	Li belt	PVDF-HFP-PI-LiTF-TEGDME	121 cycles 269 mAh·g ⁻¹	Bendable	[122]
	KB-MnO	Carbon paper	Li wire	TEGDME-EDA-LiClO ₄	235 cycles 500 mAh·g ⁻¹	Bendable	[114]
	N-CNT	SS	Li rod	PVDF-HFP/ETPTA-LiTF-TEGDME	126 cycles 1000 mAh·g ⁻¹	Bending for 5000 cycles	[75]
	Aligned CNT sheets	N/A	Lithiated Si/CNT fiber	PVDF-HFP/TMPET-LiTF-TEGDME	100 cycles 500 mAh·g ⁻¹	Bending for 20,000 cycles	[46]
Al–O ₂ battery	Ag nanoparticle	Aligned CNT sheets	Al spring	PVA-PEO-KOH	Primary 935 mAh·g ⁻¹	Stretching by 30%	[71]
	CNT paper	Ag-coated Cu wire	Al wire	PBS	N/A	Bendable	[98]
Ga/In–O ₂ battery	Pt	Carbon fiber yarn	Liquid metal (Ga/In)	PAA-KOH	primary 214.8 mAh·g ⁻¹	Stretching by 100%	[91]
Li–CO ₂ battery	N-CNT	Ti wire	Li wire	PVDF-HFP-TMPET-LiTFSI	45 cycles 1000 mAh·g ⁻¹	Bendable	[78]

To address this problem, by replacing the thick Li anode with CNT-based Si anode and employing an ultra-thin air cathode, 1D Li-air batteries with minimized diameter of ~400 μm were successfully constructed [46]. These compact 1D Li-air batteries could be woven into dense yet soft textiles through the traditional weaving/knitting techniques and bear various deformations such as bending, folding and twisting (Fig. 9b and c). Besides, series/parallel connections of battery fibers could also be achieved in a convenient manner to adjust the output voltage and current in textiles.

Integrating compliant fiber-shaped metal-air batteries with other functional systems, such as energy conversion modules, biomedical sensors and luminescent devices, could endow the integral system with self-powering feature, further expanding their scopes of applications [20]. As a typical paradigm, a self-powering smart fabric was achieved by integrating 1D dye-sensitized solar cell as the energy harvester, 1D Li–CO₂ batteries as the energy storage part and a flexible breath sensor (Fig. 9d) [46]. The real-time current response conformed to human breath showed periodic change trend during approximately 600 s, demonstrating quick response capability and stable reproducibility (Fig. 9e). Due to the theoretically higher energy density, integrated system using 1D metal-air batteries may demonstrate a more compact device size with efficient utilization of other functional components. In this regard, 1D metal-air batteries have been successfully integrated with wearable LED display, smart watch and various sensors for flexible, and even all-textile-based multi-functional platforms [21].

8. Conclusions and perspectives

In conclusion, to seek approaches for powering the burgeoning flexible electronic devices in an uninterrupted manner, a lot of efforts have been devoted to developing fiber-shaped metal-air batteries, which are highly flexible and theoretically endowed with high energy densities. In this review article, we have highlighted the recent advances of flexible, fiber-shaped metal-air batteries with an emphasis on the design of

flexible electrodes, electrolyte exploitation, and encapsulation of the fiber-shaped metal-air batteries, as summarized at Table 1. We conclude this work with some perspectives on the remaining challenges and future directions as follows:

Electrochemical performances. Despite of achievements in squeezing the capacity and enhancing the cycling performance, the fiber-shaped metal-air batteries are still far from fully unlocking their high theoretical energy densities. This can be attributed to the unique fiber-shaped configuration, which demonstrates desirable flexibility but in the meanwhile erects obstacles for performance enhancement. First, the 1D structure with high curvature interface can result in the exfoliation of active materials in electrodes, thus limits the mass loading of active materials and deactivates the utilization of electrodes. Relatively lower capacities of individual fiber-shaped metal-air batteries were obtained compared with their flexible planar counterparts [19,20]. Regarding this, a tradeoff between the mass loading of active materials and the device flexibility is required to further improve the energy-storing capability of individual 1D metal-air batteries. Second, the large aspect ratio of 1D metal-air batteries results in a common and big problem, i.e., the electrochemical performances may sharply decay with the increasing battery length due to the rapidly increased resistance along the fiber and low round-trip energy efficiency. Employing metallic 1D current collectors to gain high electrical conductivity and developing novel *in-situ* fabrication methods with decreased interface resistances are two typical strategies to maintain electrochemical performances upon extending the battery length. Despite of above achievements, to our best knowledge, the maximal lengths of metal-air battery fibers were ~50 cm, which is still far away from the demands for the continuous weaving/knitting process. In addition, the stable electrochemical performances under continuous deformations should also be more carefully considered for 1D metal-air batteries, aiming at real applications.

Safety. Another challenge at the forefront of fiber-shaped metal-air batteries is the safety issue. As we discussed before, most fiber-shaped metal-air batteries use metal wires/rods as their anodes. These metal

anodes, especially some alkali metals like Li, become one of the safety vulnerabilities of resulting battery fibers, as the inevitable dendrite formation of 1D anode is likely to pierce through the separator or gel electrolyte layer and cause short circuits. In particular, under deformations that often occurs to 1D metal-air batteries, cracks may appear on the surface of Li metal to exacerbate the dendrite growth, clouding the implementation of fiber-shaped metal-air batteries toward flexible electronics [85]. Reducing the excessive use of metal (e.g., Li), like introducing flexible substrate and fabricating alloy to replace metallic wire anodes, represents a promising strategy to alleviate the problem. Nevertheless, to the best of our knowledge, nearly all reported fiber-shaped metal-air batteries contained an excessive metal anode (e.g., anode/cathode capacity ratio > 200). Compared with the intensive investigation in air cathodes, more efforts should be devoted to enhancing the safety of 1D metal anodes, which may soon become the major bottleneck for fiber-shaped metal-air batteries. Furthermore, metal anodes will consume the electrolyte and result in side reactions, which further causes the capacity decay and serious hazards. Gel polymer electrolytes that can protect 1D metal anodes from the corrosion of moisture or CO₂ in air as well as prevent the leakage of electrolyte, have been proved feasible. Considering the complex application scenarios (e.g., at elevated temperatures) of fiber-shaped metal-air batteries, gel polymer electrolytes with higher durability like thermal stability are highly desired.

Scalable production and practical applications. To achieve large-scale and low-cost fabrication of fiber-shaped batteries, the preparation of 1D electrodes with simple, controllable and rapid procedures should be realized first. For instance, during the preparation of air cathodes, compared with the *in-situ* synthesis strategy, the spray/cast-coating methods have no advantages on enhancing electrical conductivities and designing deformable architectures for flexible electrode fibers. Nevertheless, they demonstrate a leading superiority of simple procedures and mild synthetic conditions, which are beneficial for large-scale productions of 1D electrodes. Besides, effective evaluation standards for electrochemical performances should be established. The reported energy densities of 1D metal-air batteries are generally calculated based on the mass of air cathode instead of the total mass of fiber device. The latter one is more important for real applications. After all, to be a commercially viable battery candidate for future flexible electronics, the practical energy density is even more important than its advertised advancements.

The metal-air batteries in fiber shape with good flexibility are moving towards the next step on remarkable electrochemical performance, continuous production and low cost. It can be envisioned that these metal-air batteries with unique 1D configuration will achieve their high theoretical energy densities and scalable productions, thus opening up a revolutionary direction for the development of flexible electronics in the future.

Declaration of competing interest

The authors declare that they have no known competing financial interests or personal relationships that could have appeared to influence the work reported in this paper.

Acknowledgements

This work was supported by MOST (2016YFA0203302), NSFC (21634003, 51573027 and 21604012) and STCSM (16JC1400702 and 18QA1400700).

References

- [1] P. Tan, B. Chen, H. Xu, H. Zhang, W. Cai, M. Ni, M. Liu, Z. Shao, *Energy Environ. Sci.* 10 (2017) 2056–2080.
- [2] P. Gu, M. Zheng, Q. Zhao, X. Xiao, H. Xue, H. Pang, *J. Mater. Chem.* 5 (2017) 7651–7666.

- [3] J. Pan, Y. Xu, H. Yang, Z. Dong, H. Liu, B. Xia, *Adv. Sci.* 5 (2018), 1700691.
- [4] W. Yan, C. Dong, Y. Xiang, S. Jiang, A. Leber, G. Loke, W. Xu, C. Hou, S. Zhou, M. Chen, R. Hu, P. Shum, L. Wei, X. Jia, F. Sorin, X. Tao, G. Tao, *Mater. Today* (2019), <https://doi.org/10.1016/j.mattod.2019.11.006>.
- [5] L. Wang, D. Chen, K. Jiang, G. Shen, *Chem. Soc. Rev.* 46 (2017) 6764–6815.
- [6] L. Kang, M. Weng, C. Jheng, C. Tseng, S. Ramesh, A. Gureja, H. Hsu, C. Yeh, *Procedia Comput. Sci.* 56 (2015) 104–110.
- [7] E. Huitema, *Inf. Disp.* 28 (2012) 6–10.
- [8] A. Facchetti, C. Hsiao, E. Huitema, P. Inagaki, *Inf. Disp.* 32 (2016) 6–11.
- [9] Y. Cao, Y. Tan, S. Li, W. Lee, H. Guo, Y. Cai, C. Wang, B. Tee, *Nat. Electron.* 2 (2019) 75–82.
- [10] R. Feiner, T. Dvir, *Nat. Rev. Mater.* 3 (2017) 17076.
- [11] A. Bansal, F. Yang, T. Xi, Y. Zhang, J. Ho, *Proc. Natl. Acad. Sci. U.S.A.* 115 (2018) 1469–1474.
- [12] S. Niu, N. Matsuhisa, L. Beker, J. Li, S. Wang, J. Wang, Y. Jiang, X. Yan, Y. Yun, W. Burnett, A. Poon, J. Tok, X. Chen, Z. Bao, *Nat. Electron.* 2 (2019) 361–368.
- [13] B. Yao, J. Zhang, T. Kou, Y. Song, T. Liu, Y. Li, *Adv. Sci.* 4 (2017), 1700107.
- [14] L. Mao, Q. Meng, A. Ahmad, Z. Wei, *Adv. Energy Mater.* 7 (2017), 1700535.
- [15] P. Yu, Y. Zeng, H. Zhang, M. Yu, Y. Tong, X. Lu, *Small* 15 (2019), 1804760.
- [16] Z. Lei, P. Wu, *Nat. Commun.* 9 (2018) 1134.
- [17] A. Yetisen, J. Hurtado, B. Ünal, A. Khademhosseini, H. Butt, *Adv. Mater.* 30 (2018), 1706910.
- [18] A. Zamarayeva, A. Ostfeld, M. Wang, J. Duey, I. Deckman, B. Lechêne, G. Davies, D. Steingart, A. Arias, *Sci. Adv.* 3 (2017), e1602051.
- [19] H. Sun, Y. Zhang, J. Zhang, X. Sun, H. Peng, *Nat. Rev. Mater.* 2 (2017) 17023.
- [20] X. Xu, S. Xie, Y. Zhang, H. Peng, *Angew. Chem. Int. Ed.* 131 (2019) 13778–13788.
- [21] Y. Zhu, X. Yang, T. Liu, X. Zhang, *Adv. Mater.* (2019), 1901961.
- [22] F. Mo, G. Liang, Z. Huang, H. Li, D. Wang, C. Zhi, *Adv. Mater.* (2019) 1902151.
- [23] D. Dubal, N. Chodankar, D. Kim, P. Romero, *Chem. Soc. Rev.* 47 (2018) 2065–2129.
- [24] G. Nagaraju, S. Chandra Sekhar, L. Krishna Bharat, J.S. Yu, *ACS Nano* 11 (2017) 10860–10874.
- [25] A. Sumboja, J. Liu, W. Zheng, Y. Zong, H. Zhang, Z. Liu, *Chem. Soc. Rev.* 47 (2018) 5919–5945.
- [26] W. Weng, J. Yang, Y. Zhang, Y. Li, S. Yang, L. Zhu, M. Zhu, *Adv. Mater.* (2019), 1902301.
- [27] Z. Peng, S. Freunberger, Y. Chen, P. Bruce, *Science* 337 (2012) 563–566.
- [28] L. Grande, E. Paillard, J. Hassoun, J. Park, Y. Lee, Y. Sun, S. Passerini, B. Scrosati, *Adv. Mater.* 27 (2015) 784–800.
- [29] Q. Liu, Z. Pan, E. Wang, L. An, G. Sun, *Energy storage mater.* <https://doi.org/10.1016/j.ensm.2019.12.011>.
- [30] Z. Chang, J. Xu, X. Zhang, *Adv. Energy Mater.* 7 (2017), 1700875.
- [31] J. Yi, S. Guo, P. He, H. Zhou, *Energy Environ. Sci.* 10 (2017) 860–884.
- [32] L. Ma, S. Chen, Z. Pei, Y. Huang, G. Liang, F. Mo, Q. Yang, J. Su, Y. Gao, J. Zapien, C. Zhi, *ACS Nano* 12 (2018) 1949–1958.
- [33] H. Song, H. Deng, C. Li, N. Feng, P. He, H. Zhou, *Small Method.* 1 (2017), 1700135.
- [34] J. Zhang, B. Sun, Y. Zhao, A. Tkacheva, Z. Liu, K. Yan, X. Guo, A. McDonagh, D. Shanmukaraj, C. Wang, T. Rojo, M. Armand, Z. Peng, G. Wang, *Nat. Commun.* 10 (2019) 602.
- [35] Y. Zhang, Q. Cui, X. Zhang, W.C. McKee, Y. Xu, S. Ling, H. Li, G. Zhong, Y. Yang, Z. Peng, *Angew. Chem. Int. Ed.* 55 (2016) 10717–10721.
- [36] Q. Zhu, S. Xu, Z. Cai, M. Harris, K. Wang, J. Chen, *Energy Storage Mater.* 7 (2017) 209–215.
- [37] J. Lee, S. Kim, R. Cao, N. Choi, M. Liu, K. Lee, J. Cho, *Adv. Energy Mater.* 1 (2011) 34–50.
- [38] Y. Guo, H. Li, T. Zhai, *Adv. Mater.* 29 (2017), 1700007.
- [39] L. Wang, X. Fu, J. He, X. Shi, T. Chen, P. Chen, B. Wang, H. Peng, *Adv. Mater.* (2019), 1901971.
- [40] M. Liao, H. Sun, J. Zhang, J. Wu, S. Xie, X. Fu, X. Sun, B. Wang, H. Peng, *Small* 14 (2018), 1702052.
- [41] Y. Meng, Y. Zhao, C. Hu, H. Cheng, Y. Hu, Z. Zhang, G. Shi, L. Qu, *Adv. Mater.* 25 (2013) 2326–2331.
- [42] Z. Guo, Y. Zhao, Y. Ding, X. Dong, L. Chen, J. Cao, C. Wang, Y. Xia, H. Peng, *Y. Wang, Inside Chem.* 3 (2017) 348–362.
- [43] W. Chong, J. Huang, Z. Xu, X. Qin, X. Wang, J. Kim, *Adv. Funct. Mater.* 27 (2017), 1604815.
- [44] M. Yu, X. Cheng, Y. Zeng, Z. Wang, Y. Tong, X. Lu, S. Yang, *Angew. Chem. Int. Ed.* 55 (2016) 6762–6766.
- [45] X. Li, J. Zhou, J. Zhang, M. Li, X. Bi, T. Liu, T. He, J. Cheng, F. Zhang, Y. Li, X. Mu, J. Lu, B. Wang, *Adv. Mater.* 31 (2019), 1903852.
- [46] Y. Zhang, Y. Jiao, L. Lu, L. Wang, T. Chen, H. Peng, *Angew. Chem. Int. Ed.* 56 (2017) 13741–13746.
- [47] Y. Zhang, L. Wang, Z. Guo, Y. Xu, Y. Wang, H. Peng, *Angew. Chem. Int. Ed.* 55 (2016) 4487–4491.
- [48] Z. Zhao, J. Huang, Z. Peng, *Angew. Chem. Int. Ed.* 57 (2018) 3874–3886.
- [49] T. Zhang, H. Zhou, *Nat. Commun.* 4 (2013) 1817.
- [50] P. Zhang, Y. Zhao, X. Zhang, *Chem. Soc. Rev.* 47 (2018) 2921–3004.
- [51] H. Wang, Q. Xu, *Matter.* 1 (2019) 565–595.
- [52] Q. Liu, Z. Chang, Z. Li, X. Zhang, *Small Method.* 2 (2018), 1700231.
- [53] T. Liu, Q. Liu, J. Xu, X. Zhang, *Small* 12 (2016) 3101–3105.
- [54] S. Peng, X. Han, L. Li, S. Chou, D. Ji, H. Huang, Y. Du, J. Liu, S. Ramakrishna, *Adv. Energy Mater.* 8 (2018), 1800612.
- [55] Y. Li, C. Zhong, J. Liu, X. Zeng, S. Qu, X. Han, Y. Deng, W. Hu, J. Lu, *Adv. Mater.* 30 (2018) 1703657.

- [56] J. Papp, J. Forster, C. Burke, H. Kim, A. Luntz, R. Shelby, J. Urban, B. McCloskey, *J. Phys. Chem. Lett.* 8 (2017) 1169–1174.
- [57] E. Nasybulin, W. Xu, M. Engelhard, Z. Nie, X. Li, J. Zhang, *J. Power Sources* 243 (2013) 899–907.
- [58] R. Younesi, M. Mahlin, M. Treskow, J. Scheers, P. Johansson, K. Edström, *J. Phys. Chem. C* 116 (2012) 18597–18604.
- [59] L. An, Y. Li, M. Luo, J. Yin, Y. Zhao, C. Xu, F. Cheng, Y. Yang, P. Xi, S. Guo, *Adv. Funct. Mater.* 27 (2017), 1703779.
- [60] A. Kushima, T. Koido, Y. Fujiwara, N. Kuriyama, N. Kusumi, J. Li, *Nano Lett.* 15 (2015) 8260–8265.
- [61] S. Zeng, X. Tong, S. Zhou, B. Lv, J. Qiao, Y. Song, M. Chen, J. Di, Q. Li, *Small* 14 (2018), 1803409.
- [62] F. Meng, H. Zhong, D. Bao, J. Yan, X. Zhang, *J. Am. Chem. Soc.* 138 (2016) 10226–10231.
- [63] P. Yu, L. Wang, F. Sun, Y. Xie, X. Liu, J. Ma, X. Wang, C. Tian, J. Li, H. Fu, *Adv. Mater.* 31 (2019), 1901666.
- [64] D. Ji, L. Fan, L. Li, S. Peng, D. Yu, J. Song, S. Ramakrishna, S. Guo, *Adv. Mater.* 31 (2019), 1808267.
- [65] D. Ji, L. Fan, L. Tao, Y. Sun, M. Li, G. Yang, T. Tran, S. Ramakrishna, S. Guo, *Angew. Chem. Int. Ed.* 58 (2019) 13840–13844.
- [66] X. Wang, Y. Li, T. Jin, J. Meng, L. Jiao, M. Zhu, J. Chen, *Nano Lett.* 17 (2017) 7989–7994.
- [67] M. Liu, N. Deng, J. Ju, L. Fan, L. Wang, Z. Li, H. Zhao, G. Yang, W. Kang, J. Yan, B. Cheng, *Adv. Funct. Mater.* 29 (2019), 1905467.
- [68] L. Qiu, X. Sun, Z. Yang, W. Guo, H. Peng, *Hua Hsueh Hsueh Pao* 70 (2012) 1523–1532.
- [69] M. Liao, H. Sun, X. Tao, X. Xu, Z. Li, X. Fu, S. Xie, L. Ye, Y. Zhang, B. Wang, X. Sun, H. Peng, *ACS Appl. Mater. Interfaces* 10 (2018) 26765–26771.
- [70] X. Zhang, W. Lu, G. Zhou, Q. Li, *Adv. Mater.* (2019), 1902028.
- [71] Y. Xu, Y. Zhao, J. Ren, Y. Zhang, H. Peng, *Angew. Chem. Int. Ed.* 55 (2016) 7979–7982.
- [72] Y. Xu, Y. Zhang, Z. Guo, J. Ren, Y. Wang, H. Peng, *Angew. Chem. Int. Ed.* 54 (2015) 15390–15394.
- [73] M. Thotiyl, S. Freunberger, Z. Peng, P. Bruce, *J. Am. Chem. Soc.* 135 (2013) 494–500.
- [74] G. Veith, N. Dudney, *J. Electrochem. Soc.* 158 (2011) A658–A663.
- [75] X. Yang, J. Xu, Z. Chang, D. Bao, Y. Yin, T. Liu, J. Yan, D. Liu, Y. Zhang, X. Zhang, *Adv. Energy Mater.* 8 (2018), 1702242.
- [76] J. Xu, Z. Chang, Y. Yin, X. Zhang, *ACS Cent. Sci.* 3 (2017) 598–604.
- [77] S. Nakanishi, F. Mizuno, K. Nobuhara, T. Abe, H. Iba, *Carbon* 50 (2012) 4794–4803.
- [78] Y. Li, J. Zhou, T. Zhang, T. Wang, X. Li, Y. Jia, J. Cheng, Q. Guan, E. Liu, H. Peng, B. Wang, *Adv. Funct. Mater.* 29 (2019), 1808117.
- [79] J. Zhou, X. Li, C. Yang, Y. Li, K. Guo, J. Cheng, D. Yuan, C. Song, J. Lu, B. Wang, *Adv. Mater.* 31 (2019), 1804439.
- [80] Y. Li, J. Yin, L. An, M. Lu, K. Sun, Y. Zhao, F. Cheng, P. Xi, *Nanoscale* 10 (2018) 6581–6588.
- [81] A. Wang, S. Tang, D. Kong, S. Liu, K. Chiou, L. Zhi, J. Huang, Y. Xia, J. Luo, *Adv. Mater.* 30 (2018), 1703891.
- [82] L. Ye, M. Liao, H. Sun, Y. Yang, C. Tang, Y. Zhao, L. Wang, Y. Xu, L. Zhang, B. Wang, F. Xu, X. Sun, Y. Zhang, H. Dai, P. Bruce, H. Peng, *Angew. Chem. Int. Ed.* 58 (2019) 2437–2442.
- [83] L. Ye, M. Liao, T. Zhao, H. Sun, Y. Zhao, X. Sun, B. Wang, H. Peng, *Angew. Chem. Int. Ed.* 131 (2019) 17210–17216.
- [84] Q. Yang, G. Liang, Y. Guo, Z. Liu, B. Yan, D. Wang, Z. Huang, X. Li, J. Fan, C. Zhi, *Adv. Mater.* 31 (2019), 1903778.
- [85] Y. Huang, J. Liu, X. Huang, J. Zhang, G. Yue, *Int. J. Fatig.* 78 (2015) 53–60.
- [86] K. Chandran, *Acta Mater.* 135 (2017) 201–214.
- [87] M. Stoll, K. Weidenmann, *Int. J. Fatig.* 107 (2018) 110–118.
- [88] R. Starikov, *Int. J. Impact Eng.* 59 (2013) 38–45.
- [89] X. Chen, C. Zhong, B. Liu, Z. Liu, X. Bi, N. Zhao, X. Han, Y. Deng, J. Lu, W. Hu, *Small* 14 (2018) 1702987.
- [90] H. Li, Z. Liu, G. Liang, Y. Huang, Y. Huang, M. Zhu, Z. Pei, Q. Xue, Z. Tang, Y. Wang, B. Li, C. Zhi, *ACS Nano* 12 (2018) 3140–3148.
- [91] G. Liu, J. Kim, M. Wang, J. Woo, L. Wang, D. Zou, J. Lee, *Adv. Energy Mater.* 8 (2018), 1703652.
- [92] M. Liao, J. Wang, L. Ye, H. Sun, Y. Wen, C. Wang, X. Sun, B. Wang, H. Peng, *Angew. Chem. Int. Ed.* (2019), <https://doi.org/10.1002/ange.201912203>.
- [93] H. Sun, G. Zhu, X. Xu, M. Liao, Y. Li, M. Angell, M. Gu, Y. Zhu, W. Hung, J. Li, Y. Kuang, Y. Meng, M. Lin, H. Peng, H. Dai, *Nat. Commun.* 10 (2019) 3302.
- [94] S. Wu, K. Zhu, J. Tang, K. Liao, S. Bai, J. Yi, Y. Yamauchi, M. Ishida, H. Zhou, *Energy Environ. Sci.* 9 (2016) 3262–3271.
- [95] Z. Guo, X. Dong, Y. Wang, Y. Xia, *Chem. Commun.* 51 (2015) 676–678.
- [96] G. Elia, D. Bresser, J. Reiter, P. Oberhumer, Y. Sun, B. Scrosati, S. Passerini, J. Hassoun, *ACS Appl. Mater. Interfaces* 7 (2015) 22638–22643.
- [97] X. Lin, Q. Kang, Z. Zhang, R. Liu, Y. Li, Z. Huang, X. Feng, Y. Ma, W. Huang, *J. Mater. Chem.* 5 (2017) 3638–3644.
- [98] G. Fotouhi, C. Ogier, J. Kim, S. Kim, G. Cao, A. Shen, J. Kramlich, J. Chung, *J. Micromech. Microeng.* 26 (2016), 055011.
- [99] J. Lai, Y. Xing, N. Chen, L. Li, F. Wu, R. Chen, *Angew. Chem. Int. Ed.* (2019), <https://doi.org/10.1002/anie.201903459>.
- [100] X. Cheng, J. Pan, Y. Zhao, M. Liao, H. Peng, *Adv. Energy Mater.* 8 (2018) 1702184.
- [101] Q. Zhang, K. Liu, F. Ding, X. Liu, *Nano. Res.* 10 (2017) 4139–4174.
- [102] S. Wu, J. Yi, K. Zhu, S. Bai, Y. Liu, Y. Qiao, M. Ishida, H. Zhou, *Adv. Energy Mater.* 7 (2017), 1601759.
- [103] S. Wu, Y. Qiao, S. Yang, M. Ishida, P. He, H. Zhou, *Nat. Commun.* 8 (2017) 15607.
- [104] A. Sumboja, X. Ge, Y. Zong, Z. Liu, *Funct. Mater. Lett.* 9 (2016), 1630001.
- [105] Z. Wang, H. Li, Z. Tang, Z. Liu, Z. Ruan, L. Ma, Q. Yang, D. Wang, C. Zhi, *Adv. Funct. Mater.* 28 (2018), 1804560.
- [106] F. Mo, G. Liang, D. Wang, Z. Tang, H. Li, C. Zhi, *EcoMat.* 1 (2019), e12008.
- [107] G. Liang, F. Mo, Q. Yang, Z. Huang, X. Li, D. Wang, Z. Liu, H. Li, Q. Zhang, C. Zhi, *Adv. Mater.* 31 (2019), 1905873.
- [108] B. Lv, S. Zeng, W. Yang, J. Qiao, C. Zhang, C. Zhu, M. Chen, J. Di, Q. Li, *J. Energy Chem.* 38 (2019) 170–176.
- [109] A. Manthiram, X. Yu, S. Wang, *Nat. Rev. Mater.* 2 (2017) 16103.
- [110] L. Ma, S. Chen, D. Wang, Q. Yang, F. Mo, G. Liang, N. Li, H. Zhang, J. Zapfen, C. Zhi, *Adv. Energy Mater.* 9 (2019), 1803046.
- [111] J. Fu, J. Zhang, X. Song, H. Zarrin, X. Tian, J. Qiao, L. Rasen, K. Li, Z. Chen, *Energy Environ. Sci.* 9 (2016) 663–670.
- [112] J. Park, M. Park, G. Nam, J. Lee, J. Cho, *Adv. Mater.* 27 (2015) 1396–1401.
- [113] J. Shui, J. Okasinski, P. Kenesei, H. Dobbs, D. Zhao, J. Almer, D. Liu, *Nat. Commun.* 4 (2013) 2255.
- [114] X. Lei, X. Liu, W. Ma, Z. Cao, Y. Wang, Y. Ding, *Angew. Chem. Int. Ed.* 57 (2018) 16131–16135.
- [115] M. Thomas, Y. Oda, R. Tataru, H. Kwon, K. Ueno, K. Dokko, M. Watanabe, *Adv. Energy Mater.* 7 (2017), 1601753.
- [116] J. Pan, H. Li, H. Sun, Y. Zhang, L. Wang, M. Liao, X. Sun, H. Peng, *Small* 14 (2018), 1703454.
- [117] X. Dong, Y. Lin, P. Li, Y. Ma, J. Huang, D. Bin, Y. Wang, Y. Qi, Y. Xia, *Angew. Chem. Int. Ed.* 131 (2019) 5679–5683.
- [118] Q. Liu, J. Xu, D. Xu, X. Zhang, *Nat. Commun.* 6 (2015) 7892.
- [119] J. Zhang, D. Wang, W. Xu, J. Xiao, R. Williford, *J. Power Sources* 195 (2010) 4332–4337.
- [120] L. Wang, J. Pan, Y. Zhang, X. Cheng, L. Liu, H. Peng, *Adv. Mater.* 30 (2018) 1704378.
- [121] J. Amici, C. Francia, J. Zeng, S. Bodoardo, N. Penazzi, *J. Appl. Electrochem.* 46 (2016) 617–626.
- [122] Y. Yin, X. Yang, Z. Chang, Y. Zhu, T. Liu, J. Yan, Q. Jiang, *Adv. Mater.* 30 (2018), 1703791.